

Article

Influence of Coke Ratio on the Sintering Behavior of High-Chromium Vanadium-Titanium Magnetite

Songtao Yang ^{1,2}, Mi Zhou ^{1,2,*}, Weidong Tang ^{1,2}, Tao Jiang ^{1,2}, Xiangxin Xue ^{1,2} and Weijun Zhang ¹

¹ School of Metallurgy, Northeastern University, Shenyang 110819, China; yangsongtao1984@163.com (S.Y.); twdking@163.com (W.T.); jtyz@163.com (T.J.); xuexx@mail.neu.edu.cn (X.X.); zhangwj@smm.neu.edu.cn (W.Z.)

² Key Laboratory of Liaoning Province for Recycling Science of Metallurgical Resources, Shenyang 110819, China

* Correspondence: zhoumineu@163.com

Received: 12 May 2017; Accepted: 16 June 2017; Published: 22 June 2017

Abstract: High-chromium vanadium and titanium magnetite (HCVTM) sinter has poor properties. The coke ratio has an important effect on the behavior of HCVTM sintering as it affects the mineral phases in the high-chromium vanadium and titanium sinter (HCVTS) via changing the sintering temperature and atmosphere. In this work, the sintering behavior of HCVTM mixed with varying coke ratios was investigated through sintering pot tests, X-ray diffraction (XRD), gas chromatographic analysis, and mineral phase analysis. The results show that, with the increase of the coke ratio from 4.0% to 6.0%, leading to the increase of the combustion ratio of the flue gas, the vertical sintering rate and sinter productivity decrease. Meanwhile, with the change of the coke ratio, the content of magnetite, silicate, and perovskite increase, while the hematite and calcium ferrite decrease. In addition, the tumble strength and reduction ability of HCVTS decrease, and its degradation strength increase. It was found that the appropriate coke ratio for the sintering process was 5.0 wt %.

Keywords: high-chromium vanadium and titanium magnetite; sinter; mineralogical phases; carbonthermal reaction

1. Introduction

The reserve of vanadium and titanium magnetite (VTM) is estimated at over 40 billion tons worldwide. Separating and reducing the valuable components from VTM is a challenge due to the characteristics of VTM [1,2]. HCVTM contains 61.4% total iron (TFe), 1.0% V₂O₅, 0.5% Cr₂O₃, and 5.1% TiO₂. It has a higher utilization value than the vanadium and titanium magnetite in Panzhihua, China (TFe 51.2%, V₂O₅ 0.6%, TiO₂ 13.4%, Cr₂O₃ < 0.1%) [2,3]. The integrated utilization of HCVTM is extremely difficult, due to the complicated mineral composition. Currently, it is mentioned that blast furnace smelting of HCVTM is the best choice in industrial production [4,5]. Our previous work was a fundamental study to optimize the composites ratio of HCVTM before feeding it into a blast furnace [6–10]. The study focused on the basic HCVTM characteristics, sinter ratio, and metallurgical properties instead of focusing on the carbon thermal reaction in the HCVTM sintering process. During the smelting process in a blast furnace, the insufficient bonding phase, deficient intensity, and extreme degradation of the sintered ore were observed at low temperature, which severely affects the blast smelting in the blast furnace. Since coke is the main fuel in the sintering process, the change of the coke ratio can vary the atmospheric nature and temperature level of the sintered material. Additionally, the coke ratio can affect the mineral composition and structure of sintered ore, which also has a great influence on the quality of the sintered ore [11–18]. Therefore, the

study of the effect of the coke ratio in the sintering behavior of HCVTM is critical to improving the sinter quality and energy efficiency.

Therefore, in the paper, as a parallel work, the aim is to reveal the effects of the parameter of the coke ratio on HCVTS. HCVTM (from the Amur region of Russia) was used as the raw material and the effect of the coke ratio on the sintering process was studied via a sintering pot test. The sinter rate and yield were calculated first, and then the thermodynamics of the coke combustion was analyzed. Furthermore, the effects of different coke ratios on the micro-composition of the sinter were examined and the impact of the mechanism of the sinter's mineral composition on its quality was revealed. Finally, the energy efficiency ratio of coke is obtained via comprehensive weighted methods.

2. Materials and Methods

2.1. Raw Materials

The HCVTM was supplied by the ARICOM Group Company (Amur, Russia). The other raw materials were supplied by Jianlong Iron and Steel Group Company (Shuangyashan, China). The chemical compositions of the HCVTM ore, the other three magnetite concentrates, shaft furnace ash, tailings after vanadium extraction (tailings), and quicklime are listed in Table 1. The chemical composition of the coke breeze for providing the coke ratio is listed in Table 2.

Table 1. Chemical compositions of the raw material (%).

Item	TFe	SiO ₂	CaO	MgO	Al ₂ O ₃	TiO ₂	V ₂ O ₅	Cr ₂ O ₃
HCVTM	61.42	2.54	0.32	1.20	2.95	5.12	1.01	0.47
Magnetite A	62.99	5.30	0.49	1.01	3.36	-	-	-
Magnetite B	63.73	3.24	1.09	3.03	2.15	-	-	-
Magnetite C	61.80	3.70	1.20	3.50	2.40	-	-	-
Shaft furnace ash	33.28	7.26	5.65	1.98	4.55	1.32	0.25	-
Tailings	30.68	16.97	2.44	2.82	1.53	9.81	1.22	-
Magnesite	-	3.50	1.20	42.0	-	-	-	-
Quicklime	-	2.52	83.07	3.50	-	-	-	-

Table 2. Proximate analysis of coke breeze and chemical compositions of the ash (mass fraction, %).

Fixed Carbon	Total Sulfur	Volatile	Ash (14.00)						Σ
			FeO	CaO	SiO ₂	MgO	Al ₂ O ₃	Others	
84.00	0.50	1.50	0.14	0.48	7.50	0.15	2.72	2.89	100.00

2.2. Sintering Pot Tests

According to the actual situation of raw material, the experimental schedule was designed and shown in Table 3. The basicity ($R = \omega(\text{CaO})/\omega(\text{SiO}_2)$) was adjusted by quicklime to 2.2 and kept fixed, the content of MgO was adjusted to 3% by magnesite, the content of SiO₂ was about 3.6%, and the addition of coke breeze was respectively 4%, 4.5%, 5%, 5.5%, and 6%. Sintering tests cover the blending, mixing, granulation, ignition, sintering, cooling, crushing, and treatment of the cooled sinter. The sinter mixture was loaded into the sinter pot after granulation, and then sintered after ignition at 1100 °C for 2 min until the end point at which the flue gas temperature reached its peak value; the sinter cake was then cooled for 20 min in the sinter pot and discharged. The sintering test parameters were kept fixed throughout the experiment, as listed in Table 4.

Table 3. Blend composition and sinter chemistry target of the sinter test (mass fraction, %).

Blends	Coke (%)	Materials (100%)						
		HCVTM	Magnetite A	Magnetite B	Magnetite C	Return Fines	Shaft Furnace Ash	Tailing
1	4.0	40	10	10	10	24	1.0	5.0
2	4.5	40	10	10	10	24	1.0	5.0
3	5.0	40	10	10	10	24	1.0	5.0
4	5.5	40	10	10	10	24	1.0	5.0
5	6.0	40	10	10	10	24	1.0	5.0

Table 4. Parameters of the sintering test.

Bed height: 700 mm	Sintering pot diameter: 320 mm
Ignition suction: 8.0 kPa	Sintering suction: 12.0 kPa
Ignition temperature: 1100 °C	Ignition time: 2 min
Height of hearth layer: 20 mm	Moisture: 7.5 ± 0.3%
Granulation time: 10 min	

2.3. Analysis Method

The metallurgical properties of HCVTS, including the tumble index (*TI*), low-temperature reduction disintegration index (*RDI*), and reducibility index (*RI*), were determined according to ISO-3271, ISO-4696, and ISO-7215 on the whole, respectively. The flue gas sample was obtained from the exhaust gas emitted after removing steam and ash at the flue gas mouth. Gas analysis was performed by an SC-6000 gas chromatography analyzer (Chongqing Chuanyi Analytical Instrument Co. Ltd., Chongqing, China).

The HCVTS samples with varying coke ratios were treated with coarse sandpaper after being encapsulated by resin, then treated with a relatively smooth frosted glass panel and polished in a polishing machine. Mineralogical analysis of the samples was performed with a Leica DM1750M metallographic microscope (Leica, Wetzlar, Germany) and SSX-550 scanning electron microscope (Shimadzu, Kyoto, Japan).

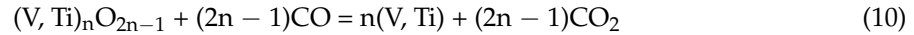
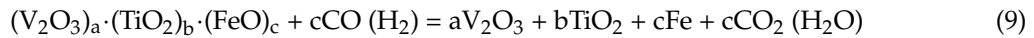
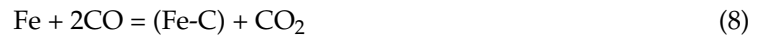
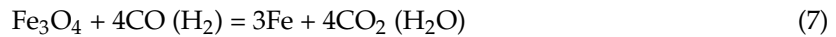
3. Results and Discussion

3.1. Flue Gas

Figure 1 shows the variation of O₂, CO, and CO₂ in flue gas during the sintering process. On one hand, it is obvious that the content of CO and CO₂ increased firstly, and then decreases at the time of 6–9 min before the end of the sintering. On the other hand, CO₂ disappeared 1–3 min later than the CO. In addition, the content of O₂ decreased gradually in the sintering process, and it increases quickly at the end of the sintering.

With an increase in the coke ratio in the sintering mixture, the content of CO increased. After extracting air and ignition, the carbon in the fuel of the sintering mixture can ignite when the temperature increases to above 700 °C. The major reactions between VTM and the reduction coal are volatilization, carbon-solution loss, carbon-stream reactions, metal-oxide reduction, and carburization. The chemical formulas representing these possible main reactions are as follows.





In the layer of sintering materials, Equations (1) and (2) are likely to occur. It should be pertinent that Equation (1) is favorable for the maximum temperature zone during the sintering process. However, the temperature of flue gas passing the pre-heat dry zone decreased rapidly due to the narrow high-temperature combustion zone. Consequently, Equation (1) is restrained. On the other hand, Equation (2) is the basic combustion reaction of carbon in the layer of the sintering material. Equation (2) releases the highest heat per unit weight of carbon, which is less affected by temperature. There is a possibility of reverse reactions at relatively low temperatures. Equations (3) and (4) are the possible reverse reactions occurring during sintering. Hence, the waste gas consists mainly of amounts of CO_2 , small amounts of CO , and free oxygen during the sintering process.

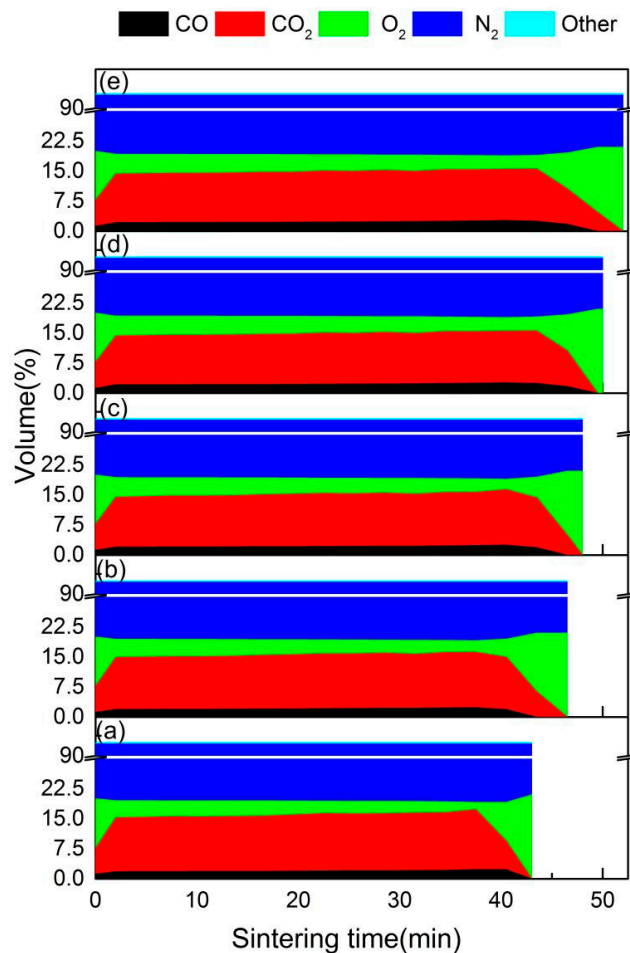


Figure 1. Variation of flue gas during sintering process. (a) C = 4.0%; (b) C = 4.5%; (c) C = 5.0%; (d) C = 5.5%; and (e) C = 6.0%.

Equation (5) may also occur during combustion of solid fuel. In the temperature range of 1000–1300 °C, the completion time of the aforementioned reaction between H_2O and C was found to be 1.5–3 s according to the chemical calculation. However, under the condition of combustion, the calculated residence time of gas in maximum temperature zone was 8–10 s. Therefore, the gas acts fully

during the combustion. The combustion of the mixed explosive gas is the main reason for obtaining a high temperature within the zone.

The reasons of the generation of CO during the sintering process were the incomplete combustion of carbon (including the low reaction temperature of Equation (1)), the reaction between C and CO₂, the direct reduction of oxides (Equations (7)–(10)), and the water gas equation (Equation (6)). Thus, the contents of CO increased with the increasing coke ratio as all of the aforementioned reactions were enhanced, especially the one between C and CO₂. CO disappears earlier than CO₂ due to the reverse reaction of Equation (4) and the over-cooling of Equation (2).

Figure 2 shows the combustion ratio of flue gas ($\text{CO}/(\text{CO} + \text{CO}_2)$) with different coke ratios. With an increase in the coke ratio, the combustion ratio of the flue gas increased, indicating the increase of the temperature in the combustion zone. During the sintering process of HCVTM, the excessive formation of perovskite at a high combustion temperature deteriorates the sintered ore quality. In this circumstance, the coke ratio in the sintering process of HCVTM should not be too high.

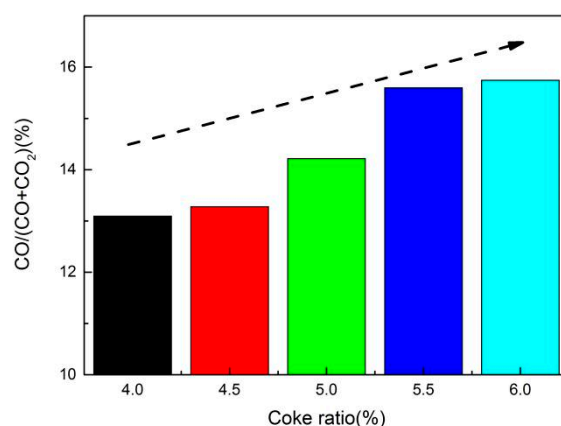


Figure 2. Combustion ratio of flue gas with different coke ratios.

3.2. Sintering Process Parameters

The effect of coke ratio on the HCVTS speed, yield, productivity, and peak temperature of the flue gas, which could reflect the level of the temperature in the sintering process indirectly, are shown in Figure 3.

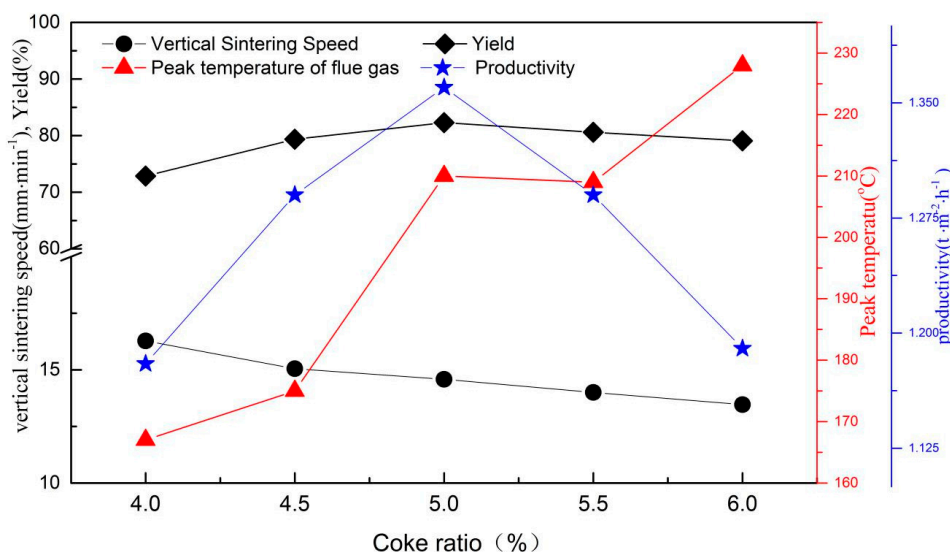


Figure 3. Effect of the coke ratio on the HCVTS sintering process.

As shown in Figure 3, by increasing the coke ratio, the vertical sintering speed decreased from 16.28 to $13.46 \text{ mm} \cdot \text{min}^{-1}$, the yield increased from 72.87% to 82.28% at a coke ratio of 5.0% , which then dropped to 79.08% . The productivity had the same trend as that of the yield, increasing from 1.18 to $1.36 \text{ t} \cdot (\text{m}^2 \cdot \text{h})^{-1}$, then dropping to $1.19 \text{ t} \cdot (\text{m}^2 \cdot \text{h})^{-1}$, while the peak temperature of flue gas increased quickly from 167 to $228 \text{ }^\circ\text{C}$, which could help us infer that the sintering temperature rises rapidly.

When the fuel level is increased from 4% to a ratio of 6% , more fuel is burned to provide more heat, so there is more liquid phase formation, which will result in a decrease of the permeability of the HCVTS mixture layer. At the same time, more fuel combustion consumes more oxygen and reduces the flow rate of the gas through the material layer due to the decrease of the permeability of the material layer, thus reducing the oxygen potential of the sintering mixture layer and the fuel reaction activity. In particular, the ratio of coke breeze increased to 6% , the unburned coke breeze appeared (Figure 4), and the sintering rate had a further drop to $13.46 \text{ mm} \cdot \text{min}^{-1}$.

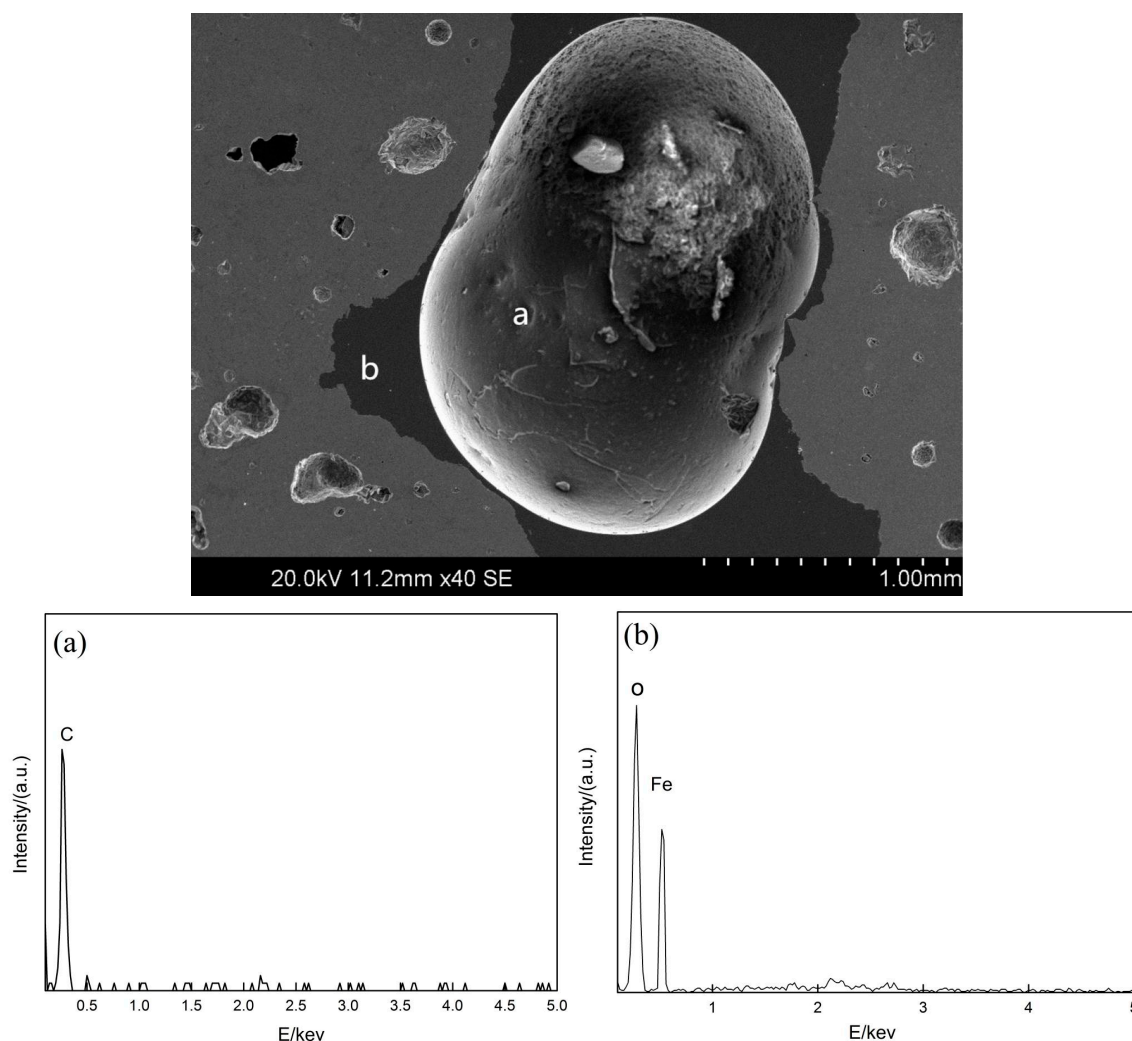


Figure 4. SEM photos of unburned coke in HCVTS. (a) EDS of point a; (b) EDS of point b.

3.3. Mineralogy

To determine the effect of the coke ratio on the HCVTS, samples with different coke ratios were analyzed by XRD and characterized using an optical microscope. To ensure the accuracy of the analytical data, the total statistical view was the total area of 100 statistical views in each sample observed via zooming in on 200 multiples with a moving step of 0.5 mm under the optical microscope.

Figure 5 shows the XRD patterns of the five sinters obtained using coke ratios of 4.0%, 4.5%, 5.0%, 5.5%, and 6.0%, respectively.

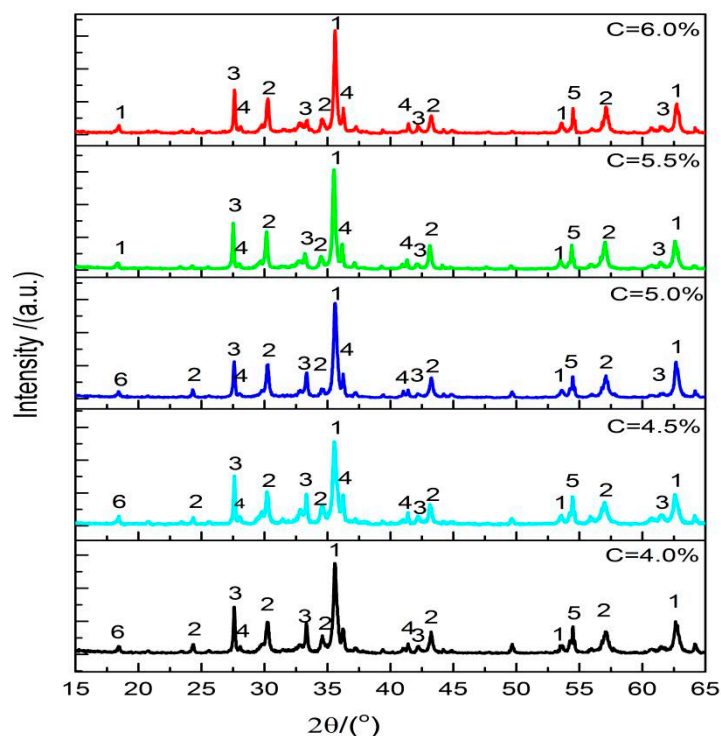


Figure 5. XRD of HCVTS at different coke ratios. 1. magnetite; 2. hematite; 3. calcium ferrite; 4. perovskite; 5. silicate; 6. ilmenite.

Figure 6 shows the mineralogy and microstructure of these five sinters. Figures 5 and 6 show that the compositions of the HCVTS mineral were primarily magnetite, hematite, perovskite, silicate (dicalcium silicate, Ca-Fe olivine, and glass), and calcium ferrite (block silico-ferrite of calcium and aluminum (SFCA) and SFCAI). Although the main mineral types have little variation, the mineral content changes significantly with the increasing coke ratio.

As increasing the coke ratio accelerated the reductive atmosphere during sintering, the formation of the silico-ferrite of calcium and aluminum (SFCA) bonding phase was suppressed and the quantities of perovskite and the glassy substance increased; these phenomena governed the strength of the sinter because SFCA is stronger than the other components. High sintering temperature resulted in the decomposition of SCFA, which decreased the quantities of the bonding phase and calcium ferrite and ultimately reduced the strength of the sinter. It is also confirmed in Figure 5 that the peak intensity of magnetite increases with the increasing coke ratio and, meanwhile, the peak intensity of hematite decreases.

At the same time, as the reducing atmosphere developed, fayalite ($2\text{FeO}\cdot\text{SiO}_2$) and kirschsteinite ($\text{CaO}\cdot\text{FeO}\cdot\text{SiO}_2$), which do not readily reduce during the sintering process, increased in the sinter, while the contents of easily-reducible hematite and calcium ferrite decreased. In addition, the content of hematite decreased and the content of the silicate bonding phase increased as the coke ratio increased.

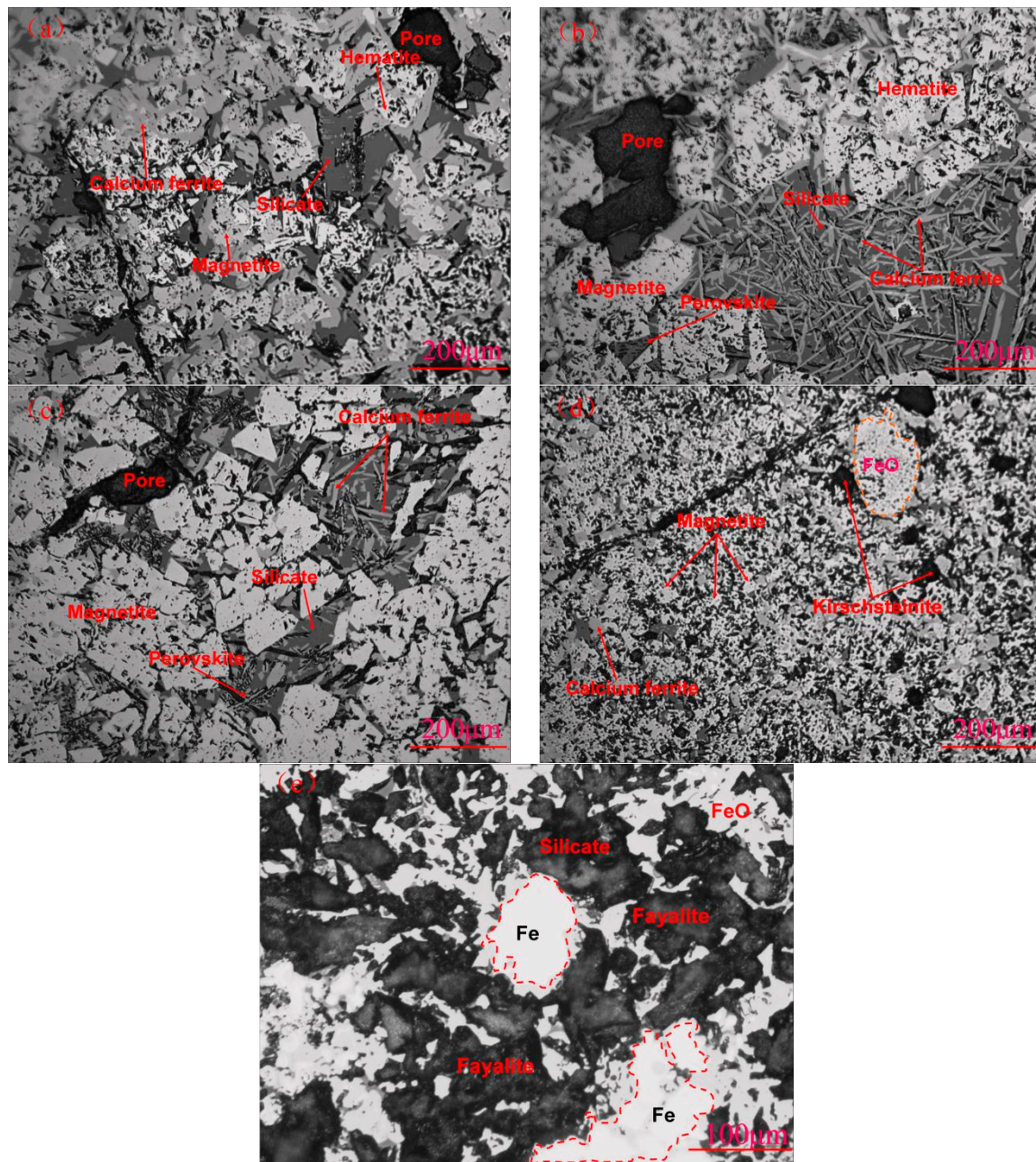


Figure 6. Mineralogy and microstructure of HCVTS at different coke ratios. (a) C = 4.0%; (b) C = 4.5%; (c) C = 5.0%; (d) C = 5.5%; and (e) C = 6.0%.

3.4. Metallurgical Performance

Figure 7 shows the metallurgical performance of the HCVTS, where TI gradually decreased from 63.89% to 60.75% with the increase of the coke ratio. From the $RDI_{+3.15}$ gradually increased from 51.86% to 67.58%, while the RI decreased from 76.98% to 73.45%. In addition, with the increase of the coke ratio from 4.0% to 6.0%, the temperature when the height of the sample reduced by 10% (T_{10}) and the temperature when the height of the sample reduced by 40% (T_{40}) were decreased from 1252 and 1362 °C to 1276 and 1392 °C, while the softening interval (ΔT) increasing from 110 to 116 °C, widens the softening range.

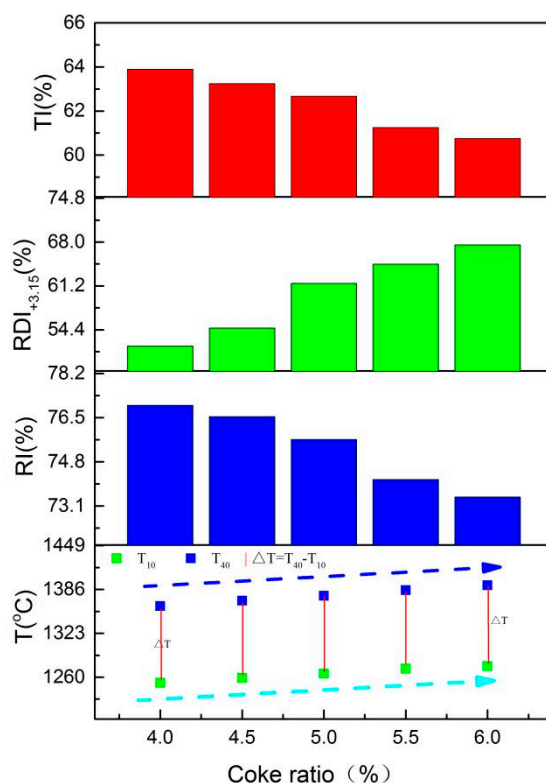


Figure 7. Effect of the coke ratio on the HCVTS metallurgical performance.

Figure 8 shows the mineral composition of the HCVTS, with the increase of the coke ratio, the sintering temperature increased, and the mineral composition of the sinter changed, the content of calcium ferrite firstly increased and then decreased, and the content of perovskite increased slightly and then increased rapidly. As the coke ratio increased to 5.0%, the heat increased, which was provided by the combustion of the carbon powder, and the liquid phase developed fully, which caused the sinter to contain a reasonable microstructure; in other words, the conditions of the mineralization of the sinter were improved and, thus, both the strength of the sinter and the rate of the finished product were enhanced. Once the coke ratio exceeded 5.0%, however, the temperature of the sinter caused excessive melt in the ore and several melting layers formed among the minerals, ferrite, and silicate phases, decreasing the content of calcium ferrite, increasing the content of perovskite, which decreased the strength and productivity of the sintered ore. The ternary phase diagram of the $\text{TiO}_2\text{-CaO-Fe}_2\text{O}_3$ system shows that the composition of calcium ferrite also changed as the temperature changed [19]. It is also indicated that the variety trend of perovskite content and calcium ferrite content were opposite at a fixed CaO content. They have an internal competitive relationship and high temperature which were beneficial to perovskite.

Moreover, volume expansion during the reduction from hematite (hexagonal lattice of the tricrystal system) to cubic magnetite (tetragonal lattice of an isometric system) is the main cause of the low-temperature reduction degradation of the sinter, and the silicate, as a bonding phase, helps to absorb the reduction phase stress of hematite during reduction. Thus, with the increase of the coke ratio, the decrease of hematite content, and the increase of silicate bonding phase content leads to the improvement of low-temperature reduction disintegration.

In addition, the increase of the coke ratio resulted in the increase of heat in the sintering process. The content of FeO and the low-melting material increased with the increase of the liquid amount, which decreased the shift of the melting point of the slag phase and the cohesive zone, improving the permeability of the soft melting performance, and widened the cohesive zone.

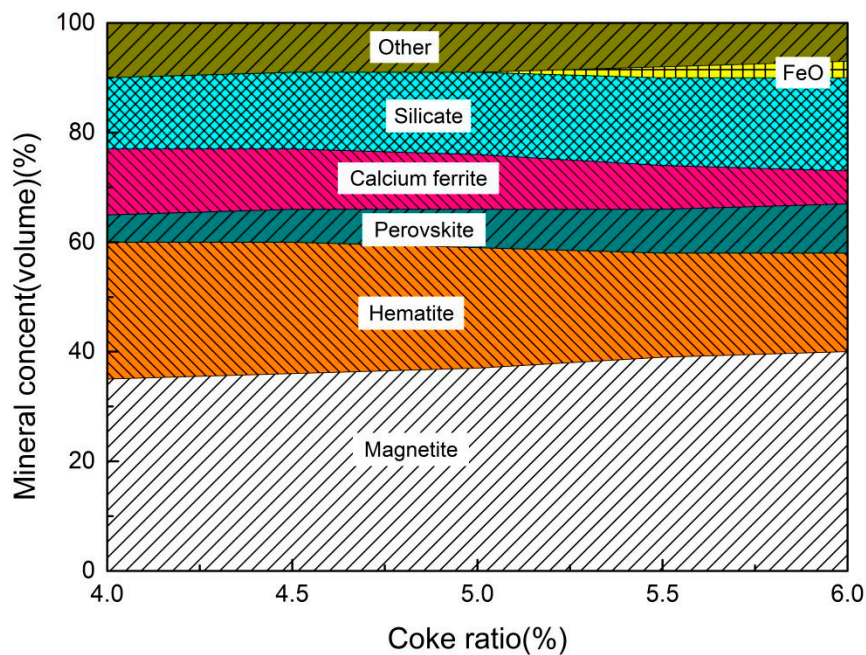


Figure 8. Effect of the coke ratio on the HCVTS mineral content.

3.5. Energy Efficiency

An appropriate coke ratio in the mixture of HCVTS can significantly improve the sinter quality and production. The subjective weights of each index are calculated by using the Delphi method [20,21], and then their objective weights can be determined by the entropy method. Finally, the optimal content of coke powder is correspondingly obtained through the comprehensive weighted methods to obtain the authentic and effective evaluation. The chosen indices (productivity, TI , RDI , and RI) and the significance coefficient were determined by the Jianglong Iron and Steel Company. Coefficient X is the evaluation matrix, Z is the standard matrix, α is the subjective weight, β is the objective weight, and the w is the comprehensive weight.

In this study, the larger the values of the productivity, TI , RDI , and RI , the better, so the larger final evaluation value, the better. The method was as follows:

First, in order to unify the trend demands of the various indices (productivity, TI , RDI , and RI), eliminate the non-commensurability among them, and obtain the evaluation of matrix $X = (x_{ij})$:

$$X = (x_{ij}) = \begin{cases} 1.18 & 63.89 & 51.86 & 76.98 \\ 1.29 & 63.24 & 54.65 & 76.54 \\ 1.36 & 62.67 & 61.58 & 75.66 \\ 1.29 & 61.25 & 64.57 & 74.12 \\ 1.19 & 60.75 & 67.58 & 73.45 \end{cases} \quad (11)$$

Second, unifying the quantitative grade of the indices to standardize and dimension X to obtain the final evaluation matrix Z .

$$Z_{ij} = 100 \times (y_{ij} - y_{ij\min}) / (y_{ij\max} - y_{ij\min}), i = 1, 2, \dots, n; j = 1, 2, \dots, m; \quad (12)$$

Define $y_{ij\min} = \min\{y_{ij} \mid i = 1, 2, \dots, n\}$, $y_{ij\max} = \max\{y_{ij} \mid i = 1, 2, \dots, n\}$.

The standardized evaluation matrix is $Z = (Z_{ij})_{nm}$:

$$Z = (Z_{ij}) = \begin{cases} 0.00 & 0.39 & 0.00 & 0.37 \\ 0.27 & 0.31 & 0.07 & 0.33 \\ 0.44 & 0.24 & 0.24 & 0.23 \\ 0.27 & 0.06 & 0.31 & 0.07 \\ 0.02 & 0.00 & 0.38 & 0.00 \end{cases} \quad (13)$$

Next, setting the significance coefficient of each index, $\alpha = (\alpha_1, \alpha_2, \dots, \alpha_m)^T$.

Define:

$$\sum_{j=1}^m \alpha_j = 1, \alpha_j \geq 0 \quad (j = 1, 2, \dots, m) \quad (14)$$

In this study, there are four indices (productivity, TI, RDI, and RI) and the significance coefficients of them are $\alpha_1 = 0.1$, $\alpha_2 = 0.3$, $\alpha_3 = 0.5$, and $\alpha_4 = 0.1$, respectively, and $\alpha = [0.1, 0.3, 0.5, 0.1]^T$.

Secondly, the objective weight of each index is determined by the entropy method:

$$B = [0.30, 0.24, 0.37, 0.23]^T \quad (15)$$

Thirdly, the preference coefficient is 0.5, and the comprehensive weight of each index is obtained:

$$W = [0.20, 0.27, 0.37, 0.17]^T \quad (16)$$

Finally, the comprehensive evaluation f_i is calculated according the following formula:

$$f_i = \sum_{j=1}^m z_{ij} w_j = 1, i = 1, 2, \dots, n \quad (17)$$

The calculation values are shown in Figure 9. The optimum energy efficiency was obtained with 5% coke.

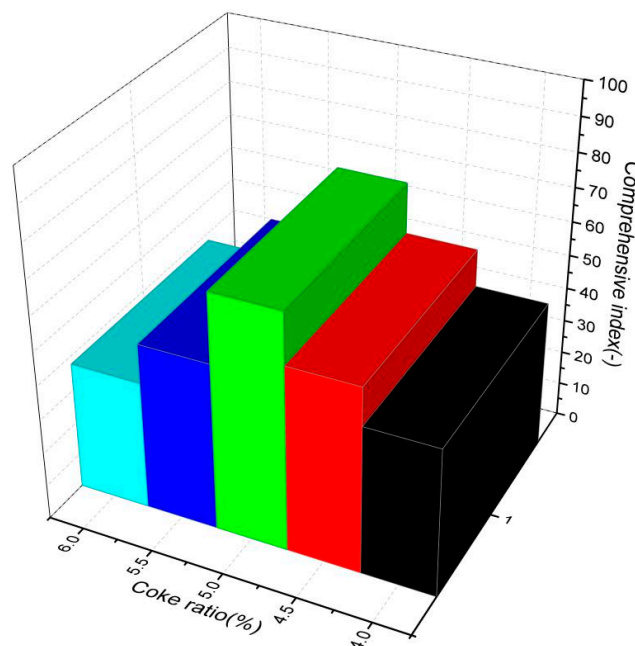


Figure 9. Effect of the coke ratio on the comprehensive index of HCVTS.

4. Conclusions

The results of this study led to the following conclusions:

- By increasing the coke ratio (from 4.0% to 6.0%), the combustion ratio of the flue gas also increased, indicating the increase in the combustion zone temperature.
- With the increase of the coke ratio, the vertical sintering rate and the ratio of sintered products decreased, and the yield increased, firstly, and then decreased.
- With different coke ratios, the mineral composition of HCVTS was found to be approximately the same. The iron-containing minerals are mainly composed of magnetite and hematite, while the bonding phase is mainly composed of calcium ferrite, silicate, and a glassy substance. In addition, the tumbler strength of HCVTS decreased; the reduction degradation performance increased while the reducibility decreased, and the appropriate coke ratio for the sintering process was found to be 5.0%.

Acknowledgments: This research was financially supported by the Programs of the National Natural Science Foundation of China (No. 51604065, 51674084, 51174051, and 5157408), the National Basic Research Program of China (973 Program) (No. 2013CB632603), the Fundamental Funds for the central universities (No. 150203003, 150202001), the Program of the National Natural Science Foundation of Liaoning Province (20170540316), and the National Key Technology R and D Program (No. 2015BAB19 B 02).

Author Contributions: Songtao Yang and Mi Zhou contributed to the material synthesis, performed the experiments, material characterization, data analysis, and paper writing; Weidong Tang revised the paper and refined the language; and Tao Jiang, Xiangxin Xue and Weijun Zhang contributed to the design of the experiment.

Conflicts of Interest: The authors declare no conflict of interest.

References

1. Du, H.G. *Principle of Smelting Vanadium-Titanium Magnetite in the Blast Furnace*; Science Press: Beijing, China, 1996; pp. 1–3.
2. Huang, R.; Lv, X.; Bai, C.; Zhang, K.; Qiu, G. Enhancement reduction of panzhihua ilmenite concentrate with coke and conglomeration of metal with ferrosilicon. *Steel Res. Int.* **2013**, *84*, 892–899. [[CrossRef](#)]
3. Zhou, L.H.; Zeng, F.H. Reduction mechanisms of vanadium-titanomagnetite-non-coking coal mixed pellet. *Ironmak. Steelmak.* **2011**, *38*, 59–64. [[CrossRef](#)]
4. Liu, J.; Cheng, G.; Liu, Z.; Chu, M.; Xue, X. Reduction process of pellet containing high chromic Vanadium–Titanium magnetite in cohesive zone. *Steel Res. Int.* **2015**, *86*, 808–816. [[CrossRef](#)]
5. Cheng, G.; Xue, X.; Jiang, T.; Duan, P. Effect of TiO₂ on the crushing strength and smelting mechanism of High-Chromium Vanadium-Titanium magnetite pellets. *Metall. Mater. Trans. B* **2016**, *47*, 1–14. [[CrossRef](#)]
6. Zhou, M.; Yang, S.T.; Jiang, T.; Xue, X.X. Influence of MgO in form of magnesite on properties and mineralogy of high chromium, vanadium, titanium magnetite sinters. *Ironmak. Steelmak.* **2015**, *42*, 217–224. [[CrossRef](#)]
7. Zhou, M.; Yang, S.T.; Jiang, T.; Xue, X.X. Influence of basicity on High-Chromium Vanadium-Titanium magnetite sinter properties, productivity, and mineralogy. *JOM* **2015**, *67*, 1–11. [[CrossRef](#)]
8. Zhou, M.; Jiang, T.; Yang, S.T.; Ma, K.; Xue, X.X.; Zhang, W.J. Optimization utilization of vanadium-titanium iron ore in sintering based on orthogonal method. *Metabank* **2016**, *55*, 581–583.
9. Zhou, M.; Jiang, T.; Yang, S.T.; Xue, X.X. Vanadium-titanium magnetite ore blends optimization for sinter strength based on iron ore basic sintering characteristics. *Int. J. Miner. Process.* **2015**, *142*, 125–133. [[CrossRef](#)]
10. Yang, S.T.; Zhou, M.; Jiang, T.; Wang, Y.J.; Xue, X.X. Effect of basicity on sintering behavior of low-titanium vanadium–titanium magnetite. *Trans. Nonferrous Met. Soc. China* **2015**, *25*, 2087–2094. [[CrossRef](#)]
11. Zhao, J.P.; Loo, C.E.; Dukino, R.D. Modelling fuel combustion in iron ore sintering. *Combust. Flame* **2015**, *165*, 1019–1024. [[CrossRef](#)]
12. Ram, P.B.; Uday, S.C.; Samir, K.S. Porosity of sinter and its relation with the sintering indices. *ISIJ Int.* **2006**, *46*, 1728–1730.
13. Eiki, K.; Yorito, S.; Takazo, K. Influence of properties of fluxing materials on the flow of melt formed in the sintering process. *ISIJ Int.* **2000**, *40*, 857–862.

14. Loo, C.E.; Wan, K.T.; Howes, V.R. Mechanical properties of natural and synthetic mineral phases in sinters having varying reduction degradation indices. *Ironmak. Steelmak.* **1988**, *15*, 279–285.
15. Inazumi, T. Influence of mineralogical characteristic of hematite in self-fluxed sinter on its degradation during the reduction. *Tetsu Hagane* **1982**, *68*, 2207–2214. [[CrossRef](#)]
16. El-Tawil, S.Z.; Morsi, I.M.; Yehia, A.; Francis, A.A. Alkali reductive roasting of ilmenite ore. *Can. Metall. Q.* **1996**, *35*, 31–37. [[CrossRef](#)]
17. Park, E.; Ostrovski, O. Reduction of the mixture of titanomagnetite ironsand and hematite Iron ore fines by carbon monoxide. *ISIJ Int.* **2004**, *44*, 214–216. [[CrossRef](#)]
18. Samanta, S.; Mukherjee, S.; Dey, R. Upgrading Metals via Direct Reduction from Poly-metallic Titaniferous Magnetite Ore. *JOM* **2015**, *67*, 467–476. [[CrossRef](#)]
19. Hohenberg, P.; Kohn, W. Inhomogeneous electron gas. *Phys. Rev. B* **1964**, *136*, 864–871. [[CrossRef](#)]
20. Zhou, M.; Yang, S.T.; Jiang, T.; Jiang, L.H.; Zhang, J.T.; Xue, X.X. Effects of carbon content on the sintering behavior of low-titanium vanadium-titanium magnetite. *Res. Technol.* **2016**, *113*, 612–622. [[CrossRef](#)]
21. Löfmark, A.; Mårtensson, G. Validation of the tool assessment of clinical education (AssCE): A study using Delphi method and clinical experts. *Nurse Educ. Today* **2016**, *50*, 82–86. [[CrossRef](#)] [[PubMed](#)]



© 2017 by the authors. Licensee MDPI, Basel, Switzerland. This article is an open access article distributed under the terms and conditions of the Creative Commons Attribution (CC BY) license (<http://creativecommons.org/licenses/by/4.0/>).